Imaging at the Nanoscale With Practical Table-Top EUV Laser-Based Full-Field Microscopes

Fernando Brizuela, Isela D. Howlett, Sergio Carbajo, Diana Peterson, A. Sakdinawat, Yanwei Liu, David T. Attwood, Mario C. Marconi, *Senior Member, IEEE*, Jorge J. Rocca, *Fellow, IEEE*, and Carmen S. Menoni, *Fellow, IEEE*

(Invited Paper)

***Abstract*—The demonstration of table-top high average power extreme-ultraviolet (EUV) lasers combined with the engineering of specialized optics has enabled the demonstration of full-field microscopes that have achieved tens of nanometer spatial resolution. This paper describes the geometry of the EUV microscopes tailored to specific imaging applications. The microscope illumination characteristics are assessed and an analysis on the microscope's spatial resolution is presented. Examples of the capabilities of these table-top EUV aerial microscopes for imaging nanostructures and surfaces are presented.**

***Index Terms*—Extreme ultraviolet (EUV) lasers, imaging, microscopy, nanotechnology.**

I. Introduction

FULL-FIELD microscopes are the most versatile and widely used instruments across many disciplines, from materials to biological science. In conventional full-field or aerial optical microscopes, the spatial resolution is limited to $\sim$200 nm by the wavelength of illumination [1]. Based on the Rayleigh criterion, the spatial resolution of an *aerial* microscope, $\mathrm{Res} = k\lambda/\mathrm{NA}_{\mathrm{obj}}$, is linearly proportional to the wavelength of the illumination λ and constant k that varies with illumination conditions and resolution test, and inversely proportional to the numerical aperture of the objective $\mathrm{NA}_{\mathrm{obj}}$ [2]–[4]. State-of-the-art full-field optical microscopes have maximized $\mathrm{NA}_{\mathrm{obj}}$ by using immersion methods and angular or structured illumination [5]. Similar techniques have been implemented in lithography with the same goal of reducing critical dimensions [6]. Pushing the resolution of full-field microscopy to tens of nanometers, as required for emerging nanoscience and nanotechnology applications is, however, a challenge.

It is possible to increase the spatial resolution of full-field microscopes beyond the limit of optical microscopes by using illumination in the extreme ultraviolet (EUV) and soft X-ray (SXR) regions of the electromagnetic spectrum. Although EUV and SXR microscopy can be considered a natural extension of conventional visible light microscopy, there are fundamental differences between the EUV/SXR and visible regions that give rise to both difficult challenges and unique opportunities. In particular, a large number of atomic resonances are present at these short wavelengths, causing most materials to strongly absorb [7]. On the other hand, the strong resonances can be exploited to enhance image contrast. The high absorption of EUV/SXR light in most materials also restricts the microscope's optics to be in the form of reflective or diffractive.

There has been significant growth in the last few years in the implementation of SXR and X-ray microscopes that use illumination generated from third- and fourth-generation synchrotron sources. In parallel, important developments in the optics have been achieved, and in combination, these SXR microscopes have reached a spatial resolution down to 12 nm [8]. A recent review describes state-of-the-art full-field X-ray imaging with synchrotron illumination [9]. At the same time, there has been significant progress in the demonstration of table-top sources of EUV/SXR light that have enabled the implementation of high-resolution imaging systems with nanometer spatial resolution at a laboratory scale [10]–[18].

Full-field microscopes based on EUV/SXR lasers were first demonstrated by Di Cicco *et al.* [19] and Da Silva *et al.* [20]. Our group has exploited the high average power of table-top EUV/SXR lasers for illumination of full-field microscopes that have achieved tens of nanometers spatial resolution [21]–[26]. The main advantages of EUV/SXR lasers are the high photon flux that is key for obtaining high-quality images with exposure times ranging from a few seconds down to a single laser shot; high monochromaticity that eliminates chromatic aberrations when using zone plate optics; and high directionality that allows us to fully collect the laser output to illuminate the sample, increasing the efficiency of the system. These properties coupled with advanced EUV/SXR optics [8], [27], [28] have made possible the implementation of practical EUV/SXR laser-based aerial microscopes.

Manuscript received January 5, 2011; revised April 1, 2011; accepted May 14, 2011. Date of publication June 2, 2011; date of current version January 31, 2012. This work was supported by the Engineering Research Centers Program of the National Science Foundation under NSF Award EEC-0310717.

F. Brizuela was with the Department of Electrical and Computer Engineering, Colorado State University, Fort Collins, CO 80523-1373 USA. He is now with the Department of Atomic Physics, Lund University, SE-221 00 Lund, Sweden.

I. D. Howlett, S. Carbajo, M. C. Marconi, J. J. Rocca, and C. S. Menoni are with the Department of Electrical and Computer Engineering and the Engineering Research Center for Extreme Ultraviolet Science and Technology, Colorado State University, Fort Collins, CO 80523-1373 USA (e-mail: c.menoni@ieee.org).

A. Sakdinawat, Y. Liu, and D. T. Attwood are with the Department of Electrical Engineering and Computer Science, University of California, Berkeley, CA 94720 USA.

D. Peterson is with the Department of Electrical and Computer Engineering, Colorado State University, Fort Collins, CO 80523-1373 USA.

Color versions of one or more of the figures in this paper are available online at http://ieeexplore.ieee.org.

Digital Object Identifier 10.1109/JSTQE.2011.2158393

This paper summarizes two main applications of EUV/SXR aerial microscopes: imaging of nanostructures and the actinic inspection of EUV lithography masks. In the first application, the short wavelength of the illumination and high photon flux have been essential to demonstrate, for the first time, single-shot full-field imaging at EUV/SXR wavelengths [24]. The second application exploits resonant illumination in the implementation of a reflection table-top actinic microscope for extreme-ultraviolet lithography (EUVL) mask inspection [25], [26]. Until now, similar systems have been implemented using synchrotron illumination [29]. In each of these applications, quantifying the illumination characteristics is key to realize diffraction limit operation of the microscope and best quality images. The second goal of this paper is to describe an analysis of the spatial coherence of the illumination that coupled with a Fourier analysis of the images allows us to fully characterize the microscopes illumination and determine their spatial resolution.

This paper is organized as follows. Section II describes transmission and reflection geometries for laser-based EUV/SXR microscopes operating at 46.9 and 13.2 nm wavelengths, respectively. In each case, the specific application dictated the optimum geometry for the microscope. Section III presents results on the characterization of spatial coherence of the illumination and spatial resolution of EUV/SXR aerial microscopes. Section IV presents specific imaging applications that have been explored.

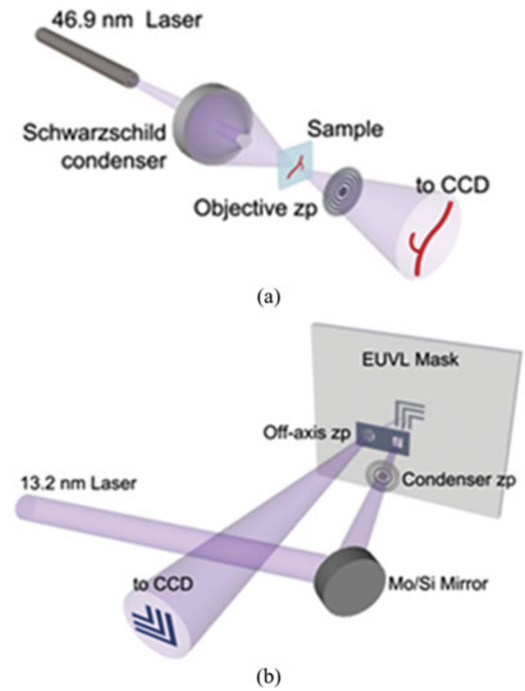

Fig. 1. (a) Schematic setup for the transmission microscope at $\lambda = 46.9$ nm. (b) Schematic setup for the reflection microscope at $\lambda = 13.2$ nm designed for the inspection of EUVL masks.

II. Geometry of a Laser-Based, EUV/SXR Full-Field Microscope

The geometry of an EUV/SXR full-field microscope operating in transmission configuration is schematically shown in Fig. 1(a). This wavelength scalable geometry has been broadly implemented using synchrotron and table-top source illumination [7], [30]. A highly collimated laser beam is collected by a condenser that illuminates the test object. A bright-field image of the object is formed on a charge-coupled array detector by a zone plate objective. We have implemented transmission microscopes using as illumination the output from EUV/SXR lasers operating at wavelengths of $\lambda = 46.9$ and 13.2 nm [21], [22], [24].

The $\lambda = 46.9$ nm microscope uses as illumination the output from a compact capillary discharge Ne-like Ar laser [11]. The laser output consists of pulses of 10 μJ energy and 1.5 ns pulse duration providing $\sim 10^{12}$ photons/pulse. The laser has been demonstrated to work at repetition rates up to 10 Hz. The laser output is highly monochromatic ($\Delta\lambda/\lambda < 1 \times 10^{-4}$) that allows the collection of images free of chromatic aberrations. Additionally, the laser output has a high degree of spatial coherence [31]. The laser produces an annular shaped beam that is completely collected by a 0.18 NA Schwarzschild condenser. The condenser's surfaces are coated with a Sc/Si multilayer, resulting in a total throughput of 13%. The condenser illuminates the sample in a geometry in which only a portion of the annular beam is used. This is done to reduce the fluence at the sample and minimize aberrations. This geometry, however, creates oblique illumination [7]. The condenser is mounted on piezo-electric motion controlled stages that allow it to move parallel to the sample plane. This is done to homogenize the illumination and reduce coherence effects on images acquired with multiple laser shots. The microscope's objective is a free-standing Fresnel zone plate with 10% efficiency in the first order. This design is used to minimize absorption at $\lambda = 46.9$ nm [32]. The characterization of the microscope presented in this paper was carried out using a 0.32 NA objective. The objective forms an $\sim 1200\times$ magnification bright-field image on an EUV/SXR-sensitive charge-coupled (CCD) array detector. The system can be reconfigured for reflection imaging. In this case, the sample is rotated 45° with respect to the illumination and the CCD detector is placed accordingly. Although there is a significant reduction in the reflectivity at grazing incidence angles larger than $\sim 20°$, the large photon flux available at $\lambda = 46.9$ nm makes it possible to acquire high-quality images with exposures of a few seconds [23]. Examples of images obtained with the microscope using $\lambda = 46.9$ nm illumination are shown in Sections III and IV.

The geometry in Fig. 1(a) was also implemented using as illumination the $\lambda = 13.2$ nm output from a laser-pumped EUV laser [12], [33]. The use of $\lambda = 13.2$ nm laser illumination, which has ~ 60% reflectivity in Mo/Si multilayer coatings used in EUVL optics and reticles, allowed the demonstration of a reflection full-field microscope for the characterization of defects in EUVL masks [25], [26].

The geometry of the $\lambda = 13.2$ nm reflection microscope was dictated by the requirement to image the mask under the same illumination conditions of a $4\times$ demagnification 0.25 NA EUVL stepper [34]. Therefore, the angle of the illumination at the mask was set to 6° and the numerical aperture of the condenser and objective was selected to be 0.0625 NA. A schematic of the microscope's geometry is shown in Fig. 1(b). The illumination was provided by the output from a laser-pumped EUV laser operating at a wavelength of $\lambda = 13.2$ nm, in the $4d^1S_0$–$4p^1P_1$ transition in Ni-like Cd [12], [33]. The laser output consists of EUV pulses of ∼200 nJ energy that, when operated at a repetition rate of 5 Hz, results in approximately 1 μW average power. The temporal coherence is high ($\Delta\lambda/\lambda < 1 \times 10^{-4}$) and the transverse coherence length is about 1/20 of the beam diameter [35]. This moderate spatial coherence makes the laser well suited for matching the illumination coherence requirements of the EUVL stepper. The microscope uses diffractive optics for the condenser and objective. The condenser and objective were designed with apertures to provide an optical path for image formation and mask illumination, respectively. Both of these nanostructured optics were fabricated by electron beam lithography [32].

The selection of the condenser and objective for the EUV/SXR full-field microscopes is critical for maximizing photon throughput, minimizing aberrations, and enabling high spatial resolution. Zone plates typically have 5–10% efficiency, and have the ability to produce aberration-free images when using the highly monochromatic illumination from the EUV/SXR lasers. The choice of a zone plate objective for the EUV/SXR microscopes is the most sensible to achieve high spatial resolution with high quality, moderate cost optics. The selection of the condenser, on the other hand, is less stringent. When suitable multilayer coatings are available at the wavelength of the illumination, a reflective condenser can offer higher throughput, and larger working distance compared to a zone plate lens. This is the case, for example, in full-field microscopes used for EUVL mask inspection that use 13.5 nm light illumination [34]. Taking into account the efficiency of the optics and other elements, such as filters that block spontaneous emission and mirrors that guide the laser output toward the condenser, and using a 50% transmissive sample, the throughput of the $\lambda = 46.9$ nm full-field transmission microscope is 6.5×10^{-3} and that of the $\lambda = 13.2$ nm reflection microscope is 4.4×10^{-4}. Based on these estimates, and taking into account that the number of photons per shot is 2.4×10^{12} and 1.3×10^{10} for $\lambda = 46.9$ and 13.2 nm illumination, respectively, a longer exposure is required at $\lambda = 13.2$ nm to capture good quality images. Experiments show that ∼20 laser shots are needed at $\lambda = 13.2$ nm while a single laser shot suffices at $\lambda = 46.9$ nm [24]. However, to extract relevant metrics on the print quality of EUVL mask, image exposure was increased six times [26]. Recent improvements in the energy output of EUV/SXR lasers at $\lambda \sim 13$ nm, project a reduction of the microscope's acquisition time to a single laser shot [36]. The nanosecond and picosecond time durations of the laser pulses at $\lambda = 46.9$ and 13.2 nm, respectively, coupled with single shot imaging capabilities make the microscopes suited for capturing the dynamics of repetitive processes in nanostructures and systems [37].

The selection of the optics also plays a significant role in the quality of the resulting images. In the next section, we describe the characterization of the microscope's illumination in terms of its degree of coherence and its influence in affecting the spatial resolution of the microscope.

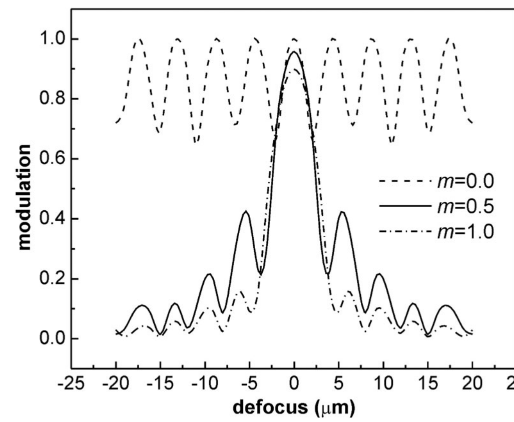

Fig. 2. Through-focus simulations of a 120-nm half-period grating imaged with a 0.061 NA objective and 13.2 nm wavelength light performed using SPLAT [39]. As the coherence of the optical system is increased (decrease in m), modulation of out-of-focus maxima increases.

III. Assessment of the Illumination Degree of Coherence and Spatial Resolution in Table-Top EUV Microscopes

The coherence properties of the illumination in a full-field microscope have a pronounced effect on the fidelity of the resulting magnified image. For microscopes based on EUV/SXR lasers, the laser's transverse coherence and the optics determine the coherence properties of the illumination. The degree of coherence of the imaging system can be evaluated using the self-imaging Talbot effect [38]. In this through-focus analysis, magnified images, replicas of a periodic grating, are obtained at distances d, termed the Talbot distance, that are equal to two times the square of the grating's period p divided by the wavelength of illumination λ. For completely coherent illumination, the images obtained at multiples of $\pm\ \frac{1}{2}\ d$ show an intensity modulation of 100%. Instead, for completely incoherent illumination, 100% intensity modulation is obtained only at the focal plane, $d = 0$. Fig. 2 shows the calculated image intensity modulation versus defocusing distance d for simulated images of a 120-nm half-pitch grating obtained with a 0.061 NA objective and $\lambda = 13.2$ nm illumination for different values of the coherence parameter m [39]. This parameter varies from completely coherent ($m = 0$) to completely incoherent ($m = 1$) [40]. The $\frac{1}{2}$ Talbot distance for this grating is $d \sim 4.4$ μm. The through-focus scan is ± 20 μm from the focal plane.

Through-focus scans were carried out for the $\lambda = 46.9$ nm transmission microscope and the $\lambda = 13.2$ nm reflection microscope by imaging 300- and 200-nm half-period gratings, respectively. Images were obtained with a single laser shot at $\lambda = 46.9$ nm while 100 shots were used at $\lambda = 13.2$ nm. The intensity modulation of these images versus defocusing distance is plotted in Fig. 3(a) and (b). The results of Fig. 3(a) show that at the first $\frac{1}{2}$ Talbot plane the intensity modulation reaches 100%, indicating that the illumination in this microscope is highly coherent, with m approaching 0. The images obtained at the first

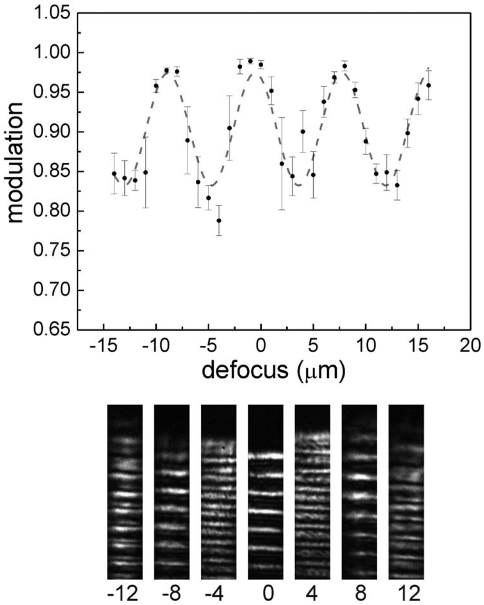

(a)

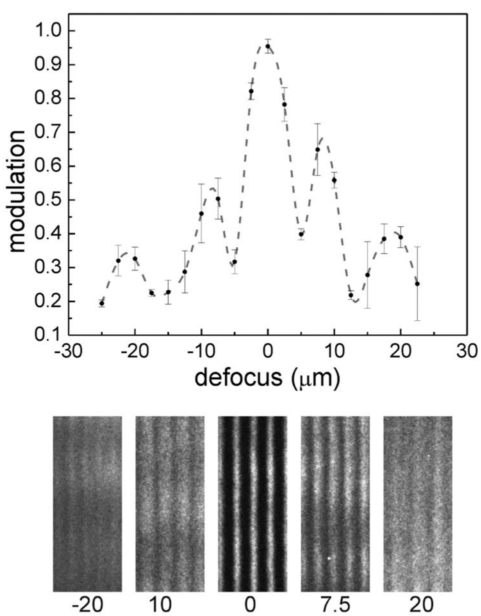

(b)

Fig. 3. (a) Through-focus modulation of a 300 nm half-pitch grating obtained with the transmission microscope with λ = 46.9 nm and an NA = 0.320 zone plate. (b) Similar analysis for a 200 nm half-pitch grating carried out with a reflection microscope at λ = 13.2 nm and with an NA = 0.0625 zone plate objective. Dashed lines added to guide the eye.

$\frac{1}{4}$ Talbot plane show the appearance of a grating with half the period of that of the object with lower modulation. The results of the through-focus analysis of Fig. 3(b) indicate a lower degree of coherence for the reflection microscope at λ = 13.2 nm. In this case, the modulation at the first $\frac{1}{2}$ Talbot plane is significantly reduced. Comparison of this curve with the calculation in Fig. 2 indicates that the illumination is partially coherent with a coherence parameter of $m \sim$0.25.

The effects of the illumination coherence on a full-field microscope are considered in the parameter k, in the expression of the Rayleigh resolution. Heck and Attwood showed that depending on the degree of coherence of the optical system and the resolution test, k varies in a nonlinear fashion with the illumination coherence and furthermore, it is resolution test dependent [40].

Based on this analysis, and for the grating test, k equals 1 and the predicted half-period grating resolution of the λ = 46.9 nm microscope is 73 nm when using a 0.32 NA objective. A similar calculation for $m = 0.25$ gives a value of k of 0.78 for the grating test which when using an $\mathrm{NA_{obj}}$ of 0.0625 predicts a half-period grating resolution of 82 nm for the reflection microscope at λ = 13.2 nm. The knife-edge resolution test for m = 1 and 0.25 predicts values that are three times smaller than those of the grating test [40].

However, there are other factors that affect the spatial resolution of an EUV full-field microscope. For example with oblique illumination, as is the case in the λ = 46.9 nm microscope, the numerical aperture of the objective is effectively increased, and hence, a higher spatial resolution can be achieved. It is possible to obtain information on the illumination conditions and extract a cutoff frequency for the imaging system through an analysis of the frequency components of images of periodic gratings obtained with the laser-based EUV microscopes.

Fig. 4 shows an EUV image of a 300-nm half-pitch transmission grating obtained with a 0.32 NA objective and λ = 46.9 nm illumination along with its Fourier components obtained by numerically taking the Fourier transform (FT) along two perpendicular directions, p and q. Both of these spectra show a cutoff frequency, taken here as the value at which the intensity in the frequency spectrum rises above the mean noise level by three times the standard deviation of the noise, 3σ. Along the p-direction, the highest spatial frequency observed is 10.5 $\mu\mathrm{m}^{-1}$, corresponding to a grating half-period of 47 nm. Instead, along the q-direction, the cutoff frequency is 5.6 $\mu\mathrm{m}^{-1}$.

The cutoff frequency is identified in Fig. 4(a) and (b) by the solid lines. Higher spatial frequency components in the p-direction are enhanced because the illumination reaches the sample at an angle of $\sim$25° from normal [7].

The results of this analysis show that the Rayleigh resolution for k = 1 and 0.32 NA [dotted line in Fig. 4(a) and (b)] underestimates the spatial resolution of the imaging system in the p-direction. The results of the FT analysis in the p-direction validate the previous independent assessment of the λ = 46.9 nm microscope spatial resolution using the grating test [24]. Furthermore, these results provide a more complete picture of the microscope's illumination.

The same image analysis was performed on images from the λ = 13.2 nm transmission and reflection microscopes. Fig. 5 shows a transmission EUV image and corresponding frequency spectrum for a 100-nm half-pitch grating imaged at λ = 13.2 nm with an NA = 0.132 zone plate. The cutoff frequency for this image is 15 $\mu\mathrm{m}^{-1}$ corresponding to a half-period grating resolution of 33 nm in agreement with previous results [22].

Fig. 6 shows the analysis for an object consisting of two orthogonal, 175-nm half-period gratings obtained with the reflection microscope using λ = 13.2 nm illumination and the

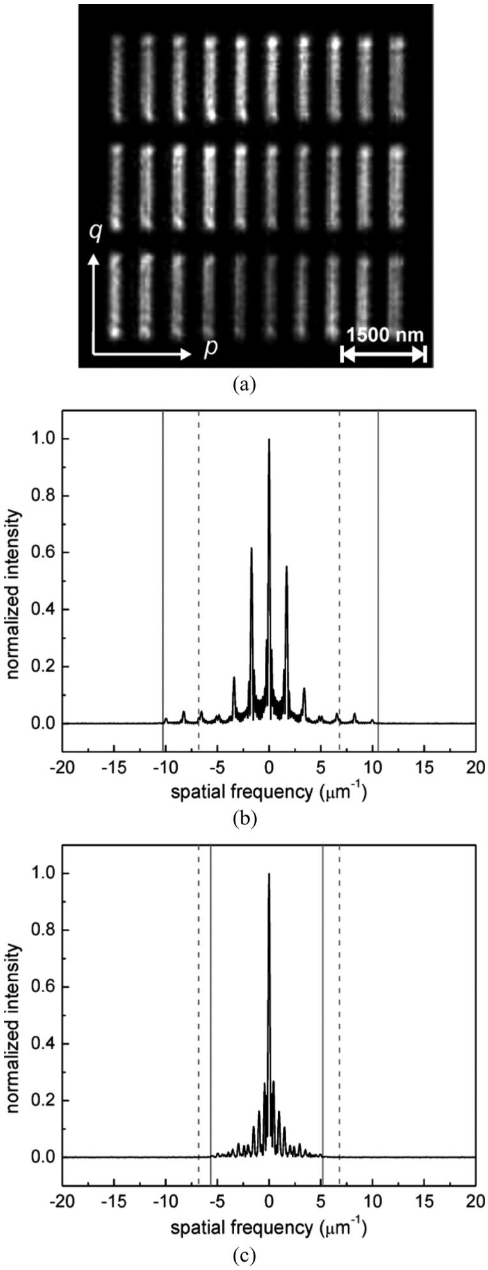

Fig. 4. (a) Single shot image of a 300-nm half-period grating obtained with the transmission microscope at 46.9 nm wavelength and a 0.32 NA objective. Fourier Transform of the image (b) along the direction of the grating, p and (c) in the perpendicular direction, q. Dotted line indicates the expected cutoff frequency considering the measured k value and the nominal NA of the objective. The solid line indicates the measured cutoff frequency.

0.0625 NA objective. The cutoff frequency in both directions is 6.7 μm^{-1}, corresponding to a grating half-period of 76 nm. The cutoff frequency is the same for both orthogonal directions because the illumination in this system is more uniform in terms of its angular spread.

The Fourier method provides a practical way of estimating the cutoff frequency in an imaging system, and could be used to improve the microscope's illumination conditions and in turn optimize its resolving power. This method complements the more rigorous grating resolution test that allows us to construct

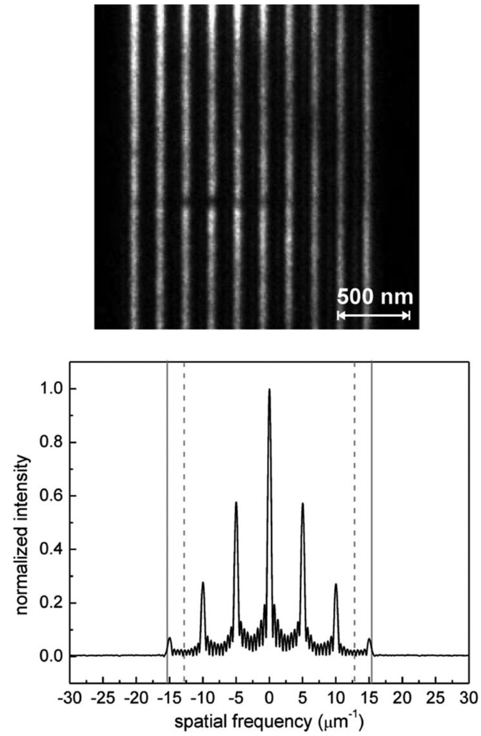

Fig. 5. Image and corresponding frequency spectrum for a 100-nm half-period transmission grating imaged at $\lambda = 13.2$ nm, with an NA $= 0.132$ zone plate. The dotted line indicates the expected cutoff frequency considering the measured k value and the nominal NA of the objective. The solid line indicates the measured cutoff frequency.

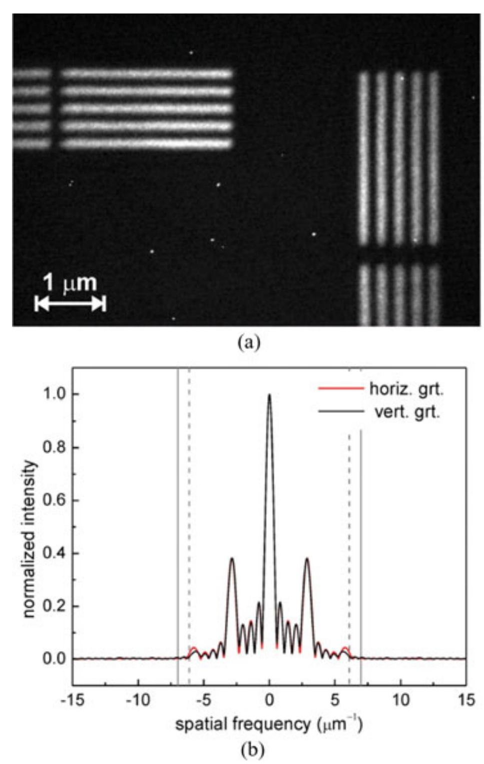

Fig. 6. Image and corresponding frequency spectra for 175-nm half-period gratings imaged at $\lambda = 13.2$ nm, with an NA $= 0.0625$ zone plate. The spectra in the two orthogonal directions are similar indicating that this system has a symmetric transfer function. The solid line indicates the measured cutoff frequency.

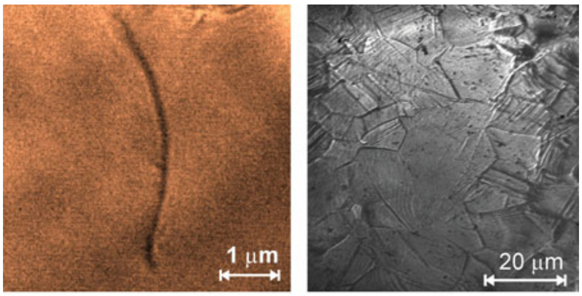

(a) (b)

Fig. 7. (a) EUV Image of a 50 nm diameter carbon nanotube on a semitransparent Si_3N_4 membrane. The image was acquired at $\lambda = 46.9$ nm, using an objective with an NA $= 0.32$ and single shot exposure. (b) EUV Image of the surface of a Zr sample where grain boundaries are visible. The image was acquired at $\lambda = 46.9$ nm, using an objective with an NA $= 0.19$ and an exposure time of 5 s.

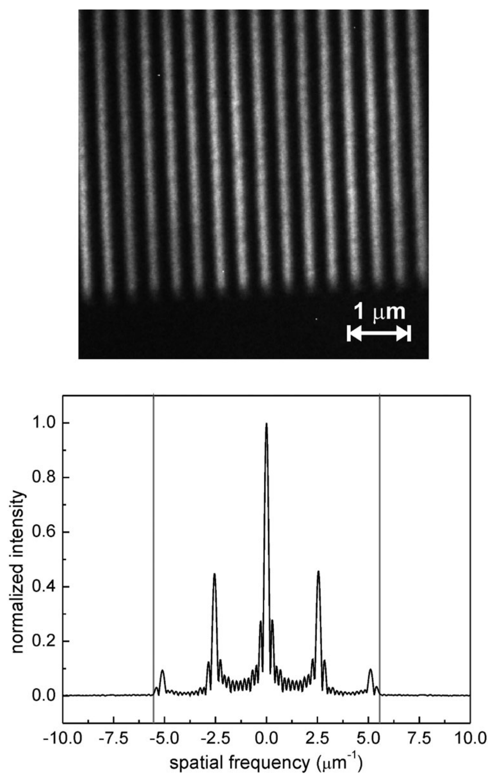

Fig. 8. EUV Image and corresponding frequency spectrum of the surface of an EUVL mask from GlobalFoundries. The lines have a half-period of 200 nm. The image was acquired at $\lambda = 13.2$ nm, using an objective with an NA $=$ 0.0625 and an exposure time of 180 laser shots to ensure sufficient intensity for image analysis. The solid lines correspond to the measured cutoff frequency.

the modulation contrast function of the microscope from the measured lineout intensity modulation from grating images with different period.

IV. Applications

The table-top EUV/SXR microscopes described here have been used to image different objects. The $\lambda = 46.9$ nm microscope was used to image nanostructures and surfaces in transmission and reflection configurations, respectively. An image of a carbon nanotube is shown in Fig. 7(a). This EUV image was obtained in transmission configuration with a single laser shot.

The flash imaging capabilities of the $\lambda = 46.9$ nm microscope provide the opportunity to record repetitive dynamic phenomena in nanoscale systems. In work in progress, we have recently demonstrated time-resolved microscopy with nanosecond temporal resolution and 50 nm spatial resolution [37]. An example of the images that can be obtained in reflection configuration is shown in the image of Fig. 7(b). This EUV image, captured with 15 laser shots' exposure, corresponds to the surface of a polished Zr pellet. The image shows well-defined grain boundaries and twins.

An EUV image obtained with the $\lambda = 13.2$–nm full-field microscope operating in a reflection mode is shown in Fig. 8. The image corresponds to the surface of an EUVL mask from GlobalFoundries containing lines with a half-pitch of 200 nm. The image was acquired using an objective with an NA $= 0.0625$ and an exposure of 180 laser shots. The recent demonstration of a tenfold increase in the laser output will enable to shorten the exposure to possibly a single laser shot. This is an encouraging step toward the implementation of a high throughput at-wavelength EUVL mask defect characterization microscope capable of capturing high-quality images with a single laser shot.

V. Conclusion

We have described in detail the implementation of full-field microscopes based on EUV/SXR laser illumination. We have also presented results on the implementation of an image analysis method that allows to characterize and optimize the microscope's illumination to realize the best resolution and image quality. The Fourier analysis can be used to determine the modulation contrast function of the microscope if the geometry of the grating is known, for example, from a scanning electron micrograph image. Capitalizing on the high throughput of the EUV/SXR-laser-based microscopes, it will be possible to implement *in situ* optimization of the illumination using the analysis described here.

Examples of the capabilities of EUV/SXR full-field microscopes to capture high-quality images of nanoscale objects with short exposure down to a single laser shot were also presented. One aspect of the illumination that has yet to be exploited is the controllable degree of spatial coherence of the illumination. This, coupled with the high throughput of the EUV/SXR laser output, will make it possible to implement geometries where phase can be exploited as in differential interference contrast imaging [28], [41], [42].

Acknowledgment

The authors would like to acknowledge the contributions of E. H. Anderson, W. Chao, A. Vinogradov, I. Artioukov, Y. P. Pershyn, and V. V. Kondratenko in EUV optics development; B. Luther, Y. Wang, D. Martz, D. Alessi, M. Grisham, and S. Heinbuch in the engineering of EUV lasers; G. Vaschenko and C. Brewer for their help in the initial development of the microscopes; and C. Tome and B. La Fontaine for providing valuable samples used for imaging.

REFERENCES

[1] Y. Garini, B. J. Vermolen, and I. T. Young, "From micro to nano: Recent advances in high-resolution microscopy," *Curr. Opin. Biotechnol.*, vol. 16, pp. 3–12, Feb. 2005.

[2] J. Goodman, *Introduction to Fourier Optics*, 3rd ed. Greenwood Village, CO: Roberts & Company, 2005.

[3] M. Born and E. Wolf, *Principles of Optics*, 7th ed. New York: Cambridge Univ. Press, 1999.

[4] E. Hecht, *Optics*, 4th ed. Reading, MA: Addison-Wesley, 2001.

[5] A. Neumann, Y. Kuznetsova, and S. R. J. Brueck, "Structured illumination for the extension of imaging interferometric microscopy," *Opt. Exp.*, vol. 16, pp. 6785–6793, May 2008.

[6] V. Bakshi, *EUV Lithography*. Bellingham, WA: SPIE, 2009.

[7] D. T. Attwood, *Soft X-Rays and Extreme Ultraviolet Radiation*. Cambridge, U.K.: Cambridge Univ. Press, 1999.

[8] W. Chao, J. Kim, S. Rekawa, P. Fischer, and E. H. Anderson, "Demonstration of 12 nm resolution Fresnel zone plate lens based soft X-ray microscopy," *Opt. Exp.*, vol. 17, pp. 17669–17677, Sep. 2009.

[9] A. Sakdinawat and D. Attwood, "Nanoscale X-ray imaging," *Nature Photon.*, vol. 4, pp. 840–848, Dec. 2010.

[10] H. T. Kim, I. W. Choi, N. Hafz, J. H. Sung, T. J. Yu, K. H. Hong, T. M. Jeong, Y. C. Noh, D. K. Ko, K. A. Janulewicz, J. Tummler, P. V. Nickles, W. Sandner, and J. Lee, "Demonstration of a saturated Ni-like Ag x-ray laser pumped by a single profiled laser pulse from a 10-Hz Ti: Sapphire laser system," *Phys. Rev. A*, vol. 77, pp. 023807-1–023807-6, Feb. 2008.

[11] S. Heinbuch, M. Grisham, D. Martz, and J. J. Rocca, "Demonstration of a desk-top size high repetition rate soft x-ray laser," *Opt. Exp.*, vol. 13, pp. 4050–4055, May 30, 2005.

[12] Y. Wang, M. A. Larotonda, B. M. Luther, D. Alessi, M. Berrill, V. N. Shlyaptsev, and J. J. Rocca, "Demonstration of high-repetition-rate tabletop soft-x-ray lasers with saturated output at wavelengths down to 13.9 nm and gain down to 10.9 nm," *Phys. Rev. A*, vol. 72, pp. 053807-1–053807-7, Nov. 2005.

[13] P. A. C. Takman, H. Stollberg, G. A. Johansson, A. Holmberg, M. Lindblom, and H. M. Hertz, "High-resolution compact X-ray microscopy," *J. Microsc.*, vol. 226, pp. 175–181, May 2007.

[14] M. Wieland, C. Spielmann, U. Kleineberg, T. Westerwalbesloh, U. Heinzmann, and T. Wilhein, "Toward time-resolved soft X-ray microscopy using pulsed fs-high-harmonic radiation," *Ultramicroscopy*, vol. 102, pp. 93–100, Jan. 2005.

[15] P. W. Wachulak, A. Bartnik, and H. Fiedorowicz, "Sub-70 nm resolution tabletop microscopy at 13.8 nm using a compact laser-plasma EUV source," *Opt. Lett.*, vol. 35, pp. 2337–2339, 2010.

[16] R. L. Sandberg, A. Paul, D. A. Raymondson, S. Hadrich, D. M. Gaudiosi, J. Holtsnider, R. I. Tobey, O. Cohen, M. M. Murnane, H. C. Kapteyn, C. G. Song, J. W. Miao, Y. W. Liu, and F. Salmassi, "Lensless diffractive imaging using tabletop coherent high-harmonic soft-x-ray beams," *Phys. Rev. Lett.*, vol. 99, pp. 098103-1–098103-4, Aug. 2007.

[17] R. L. Sandberg, D. A. Raymondson, C. La-o-Vorakiat, A. Paul, K. S. Raines, J. Miao, M. M. Murnane, H. C. Kapteyn, and W. F. Schlotter, "Tabletop soft-x-ray Fourier transform holography with 50 nm resolution," *Opt. Lett.*, vol. 34, pp. 1618–1620, Jun. 2009.

[18] H. M. Hertz, M. Bertilson, E. Chubarova, J. Ewald, S. C. Gleber, O. Hemberg, M. Henriksson, O. von Hofsten, A. Holmberg, M. Lindblom, E. Mudry, M. Otendal, J. Reinspach, M. Schlie, P. Skoglund, P. Takman, J. Thieme, J. Sedlmair, R. Tjornhammar, T. Tuohimaa, M. Vita, and U. Vogt, "Laboratory x-ray micro imaging: Sources, optics, systems and applications," in *Proc. 9th Int. Conf. X-Ray Microsc.*, 2009, J. Phys.: Conf. Ser. vol. 186, article No. 012027, doi:10.1088/1742-6596/186/1/012027.

[19] D. S. Di Cicco, D. Kim, R. Rosser, and S. Suckewer, "First stage in the development of a soft x-ray reflection imaging microscope in the Schwarzschild configuration using a soft x-ray laser at 18.2 nm," *Opt. Lett.*, vol. 17, pp. 157–159, Jan. 1992.

[20] L. B. Da Silva, J. E. Trebes, R. Balhorn, S. Mrowka, E. H. Anderson, D. T. Attwood, T. W. Barbee, J. Brase, M. Corzett, J. Gray, J. A. Koch, C. Lee, D. Kern, R. A. London, B. J. Macgowan, D. L. Matthews, and G. Stone, "X-ray laser microscopy of rat sperm nuclei," *Science*, vol. 258, pp. 269–271, Oct. 1992.

[21] G. Vaschenko, F. Brizuela, C. Brewer, M. Grisham, H. Mancini, C. S. Menoni, M. C. Marconi, J. J. Rocca, W. Chao, J. A. Liddle, E. H. Anderson, D. T. Attwood, A. V. Vinogradov, I. A. Artioukov, Y. P. Pershyn, and V. V. Kondratenko, "Nanoimaging with a compact extreme-ultraviolet laser," *Opt. Lett.*, vol. 30, pp. 2095–2097, Aug. 15, 2005.

[22] G. Vaschenko, C. Brewer, F. Brizuela, Y. Wang, M. A. Larotonda, B. M. Luther, M. C. Marconi, J. J. Rocca, and C. S. Menoni, "Sub-38 nm resolution tabletop microscopy with 13 nm wavelength laser light," *Opt. Lett.*, vol. 31, pp. 1214–1216, May 1, 2006.

[23] F. Brizuela, G. Vaschenko, C. Brewer, M. Grisham, C. S. Menoni, M. C. Marconi, J. J. Rocca, W. Chao, J. A. Liddle, E. H. Anderson, D. T. Attwood, A. V. Vinogradov, I. A. Artioukov, Y. P. Pershyn, and V. V. Kondratenko, "Reflection mode imaging with nanoscale resolution using a compact extreme ultraviolet laser," *Opt. Exp.*, vol. 13, pp. 3983–3988, May 30, 2005.

[24] C. A. Brewer, F. Brizuela, P. Wachulak, D. H. Martz, W. Chao, E. H. Anderson, D. T. Attwood, A. V. Vinogradov, I. A. Artyukov, A. G. Ponomareko, V. V. Kondratenko, M. C. Marconi, J. J. Rocca, and C. S. Menonil, "Single-shot extreme ultraviolet laser imaging of nanostructures with wavelength resolution," *Opt. Lett.*, vol. 33, pp. 518–520, Mar. 2008.

[25] F. Brizuela, Y. Wang, C. A. Brewer, F. Pedaci, W. Chao, E. H. Anderson, Y. Liu, K. A. Goldberg, P. Naulleau, P. Wachulak, M. C. Marconi, D. T. Attwood, J. J. Rocca, and C. S. Menoni, "Microscopy of extreme ultraviolet lithography masks with 13.2 nm tabletop laser illumination," *Opt. Lett.*, vol. 34, pp. 271–273, Feb. 2009.

[26] F. Brizuela, S. Carbajo, A. Sakdinawat, D. Alessi, D. H. Martz, Y. Wang, B. Luther, K. A. Goldberg, I. Mochi, D. T. Attwood, B. La Fontaine, J. J. Rocca, and C. S. Menoni, "Extreme ultraviolet laser-based tabletop aerial image metrology of lithographic masks," *Opt. Exp.*, vol. 18, pp. 14467–14473, Jul. 2010.

[27] A. Sakdinawat and Y. Liu, "Soft-x-ray microscopy using spiral zone plates," *Opt. Lett.*, vol. 32, pp. 2635–2637, Sep. 2007.

[28] A. Sakdinawat and Y. W. Liu, "Phase contrast soft x-ray microscopy using Zernike zone plates," *Opt. Exp.*, vol. 16, pp. 1559–1564, Feb. 2008.

[29] K. A. Goldberg, A. Barty, Y. W. Liu, P. Kearney, Y. Tezuka, T. Terasawa, J. S. Taylor, H. S. Han, and O. R. Wood, "Actinic inspection of extreme ultraviolet programmed multilayer defects and cross-comparison measurements," *J. Vac. Sci. Technol. B*, vol. 24, pp. 2824–2828, 2006.

[30] G. Schmahl, D. Rudolph, B. Niemann, and O. Christ, "Zone plate x-ray microscopy," *Quart. Rev. Biophys.*, vol. 13, pp. 297–315, 1980.

[31] Y. Liu, M. Seminario, F. G. Tomasel, C. Chang, J. J. Rocca, and D. T. Attwood, "Achievement of essentially full spatial coherence in a high-average-power soft-x-ray laser," *Phys. Rev. A*, vol. 6303, p. 033802, Mar. 2001.

[32] E. H. Anderson, "Specialized electron beam nanolithography for EUV and X-ray diffractive optics," *IEEE J. Quantum Electron.*, vol. 42, no. 1, pp. 27–35, Jan./Feb. 2006.

[33] J. J. Rocca, Y. Wang, M. A. Larotonda, B. M. Luther, M. Berrill, and D. Alessi, "Saturated 13.2 nm high-repetition-rate laser in nickellike cadmium," *Opt. Lett.*, vol. 30, pp. 2581–2583, Oct. 2005.

[34] A. Barty, Y. W. Liu, E. Gullikson, J. S. Taylor, and O. Wood, "Actinic inspection of multilayer defects on EUV masks," in *Emerging Lithographic Technologies IX, Parts 1 and 2*, 2005, vol. 5751, pp. 651–659.

[35] Y. Liu, Y. Wang, M. A. Larotonda, B. M. Luther, J. J. Rocca, and D. T. Attwood, "Spatial coherence measurements of a 13.2 nm transient nickel-like cadmium soft X-ray laser pumped at grazing incidence," *Opt. Exp.*, vol. 14, pp. 12872–12879, Dec. 2006.

[36] D. H. Martz, D. Alessi, B. M. Luther, Y. Wang, D. Kemp, M. Berrill, and J. J. Rocca, "High-energy 13.9 nm table-top soft-x-ray laser at 2.5 Hz repetition rate excited by a slab-pumped Ti:sapphire laser," *Opt. Lett.*, vol. 35, pp. 1632–1634, May 2010.

[37] S. Carbajo, F. Brizuela, A. Sakdinawat, Y. Liu, W. Chao, E. H. Anderson, A. V. Vinogradov, I. A. Artioukov, D. T. Attwood, M. C. Marconi, J. J. Rocca, and C. S. Menoni, "Movies at the nanoscale using extreme ultraviolet laser light," in *Frontiers in Optics*, 2010, Paper PDPB2.

[38] K. A. Goldberg, P. P. Naulleau, A. Barty, S. B. Rekawa, C. D. Kemp, R. F. Gunion, F. Salmassi, E. M. Gullikson, E. H. Anderson, and H. S. Han, "Performance of actinic EUVL mask imaging using a zoneplate microscope," in *Proc. SPIE Photomask Technology, Parts 1–3*, 2007, vol. 6730, p. 67305E.

[39] "SPLAT," [Online]. Available: http://cuervo2.eecs.berkeley.edu

[40] J. M. Heck, D. T. Attwood, W. Meyer-Ilse, and E. H. Anderson, "Resolution determination in X-ray microscopy: An analysis of the effects of partial coherence and illumination spectrum," *J. X-Ray Sci. Technol.*, vol. 8, pp. 95–104, 1998.

[41] A. Anand and B. Javidi, "Three-dimensional microscopy with single-beam wavefront sensing and reconstruction from speckle fields," *Opt. Lett.*, vol. 35, pp. 766–768, Mar. 2010.

[42] O. von Hofsten, M. Bertilson, M. Lindblom, A. Holmberg, H. M. Hertz, and U. Vogt, "Compact phase-contrast soft X-ray microscopy," in *9th Int. Conf. X-Ray Microsc.*, 2009, J. Phys.: Conf. Ser. vol. 18, article No. 012038, doi:10.1088/1742-6596/186/1/012038.

Fernando Brizuela received the B.S. degree in materials engineering from Universidad Nacional de Mar del Plata, Mar del Plata, Argentina, in 2003. He received the M.Sc. degree in electrical and computer engineering from Colorado State University, Fort Collins, in 2006. He received the Ph.D. degree in electrical and computer engineering from the same institution in 2010 for his research in high-resolution full-field microscope using table-top extreme ultraviolet laser sources.

He is currently a Postdoctoral Researcher in the Department of Atomic Physics, Lund University, Lund, Sweden.

Isela D. Howlett received the B.S. degree in optical science and engineering from the University of Arizona, Tucson, in 2010. She is currently working toward the M.Sc. degree in electrical and computer engineering at Colorado State University, Fort Collins.

She is a member of the imaging team at the National Science Foundation Engineering Research Center for Extreme Ultraviolet Science and Technology, Colorado State University. Her research interests include high-resolution imaging and image analysis methods.

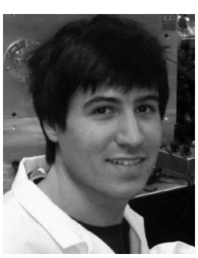

Sergio Carbajo received the M.Sc. degree in telecommunications engineering from the Engineering School, Universidad de Navarra (Tecnun), Spain, in 2009. He is currently working toward the M.Sc. degree in electrical and computer engineering at Colorado State University, Fort Collins.

He joined the National Science Foundation Engineering Research Center (EUV-ERC) for Extreme Ultraviolet (EUV) Science and Technology, Colorado State University, in 2008. His current research interests include the development of nanometer-scale spatial and temporal resolutions and laser-based EUV/soft X-ray imaging systems.

Mr. Carbajo serves as a member of the Student Leadership Council of the EUV ERC. He is also a student member of the American Physics Society, the Optical Society of America, the International Society for Optics and Photonics, and is part of the Executive Board of the IEEE Photonics Denver Chapter.

Diana Peterson is currently working towards an undergraduate degree in electrical and computer engineering at Colorado State University, Fort Collins.

In 2009 and 2010, she was part of the Research Experience for Undergraduate Program at the National Science Foundation Engineering Research Center for Extreme Ultraviolet Science and Technology, Colorado State University. She is an Honors Scholar, and will be conducting her Honors thesis in high-resolution imaging with EUV lasers.

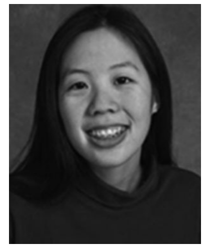

A. Sakdinawat received the Ph.D. degree in bioengineering from the University of California Berkeley and the University of California San Francisco.

She is currently a Research Scientist in the Electrical Engineering and Computer Sciences Department, University of California, Berkeley. Her research interests include nanoscale X-ray imaging at modern X-ray sources, including both lens-based and lensless imaging methods, X-ray diffractive optics, nanofabrication, and scientific applications tomagnetic, environmental, and biological materials.

Dr. Sakdinawat was awarded the Werner Meyer-Ilse Memorial International X-ray Microscopy Award in 2008.

Yanwei Liu received the B.S. degree in physics from Wuhan University, Hubei, China, in 1993, the M.S. degree in optics from the Institute of Physics, Chinese Academy of Sciences, Beijing, China, in 1996, and the Ph.D. degree in applied science and technology from the University of California, Berkeley, in 2003.

He is a Research Scientist at the University of California, Berkeley, and a member of NSF EUV ERC. His research interests include reflective and diffractive optics at EUV and soft X-ray wavelengths, and their applications in areas such as high resolution imaging and ultrafast phenomenon.

David T. Attwood received the Ph.D. degree in applied physics from New York University in 1972.

He has been a Professor in Residence at the University of California, Berkeley since 1989. He is Chair of the Applied Science and Technology Ph.D. program, and has been Principal Faculty Advisor for the undergraduate Engineering Physics program for 20 years. His research interests center on the use of short wavelength electromagnetic radiation, soft X-rays and extreme ultraviolet radiation in the 1–50 nm range. Applications of particular interest include element specific soft X-ray microscopy and EUV lithography. He was founding Director of the Center for X-Ray Optics (CXRO), Lawrence Berkeley National Laboratory, and was first (1985-1988) Scientific Director of the Advanced Light Source (ALS). He is the author of the book *Soft X-Rays and Extreme Ultraviolet Radiation: Principles and Applications* (Cambridge University Press, 2000).

Dr. Attwood is a Fellow Member of the American Physical Society and the Optical Society of America. His lectures have been broadcast live over the Internet and electronically archived at www.coe.berkeley.edu/AST/sxreuv and www.coe.berkeley.edu/AST/srms.

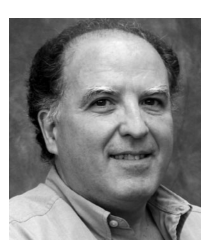

Mario C. Marconi (M'05–SM'09) received the Ph.D. degree in physics from the University of Buenos Aires, Buenos Aires, Argentina, in 1985.

He is currently a Professor in the Department of Electrical and Computer Engineering, Colorado State University, Fort Collins. He is a Faculty Member of the National Science Foundation Engineering Research Center for Extreme Ultraviolet Science and Technology, Colorado State University. His current research interests include the development of table-top extreme ultraviolet lasers and its applications in interferometry, holography, and nanopatterning.

Dr. Marconi is a Senior Member of the IEEE Photonics Society and the American Physical Society, and is a Fellow of the Optical Society of America.

Jorge J. Rocca (M'80–SM'85–F'00) received the Diploma in physics from the University of Rosario, Rosario, Argentina, in 1978, and the Ph.D. degree in electrical and computer engineering (ECE) from Colorado State University, Fort Collins, in 1983.

Since 1983, he has been a Faculty Member in the Departments of ECE and Physics, Colorado State University, where he is currently a University Distinguished Professor. His research interests include the development and physics of compact soft X-ray lasers and their applications. His group demonstrated the first gain-saturated table-top soft X-ray laser using a discharge plasma as gain medium, and later extended bright high repetition rate table-top lasers down to 10 nm using laser-created plasmas, achieving full phase coherence by injection seeding. He and his collaborators have demonstrated the use of these lasers in nanoscale imaging, dense plasma diagnostics, nanoscale material studies, and photochemistry.

Dr. Rocca is a Fellow of the American Physical Society and the Optical Society of America. He received a Distinguished Lecturer Award from the IEEE in 2006. He was also a National Science Foundation Presidential Young Investigator. He is the 2011 recipient of the 2011 Arthur L. Schawlow Prize in Laser Science.

Carmen S. Menoni (M'90–SM'99–F'10) received the Ph.D. degree in physics from Colorado State University (CSU), Fort Collins, in 1987.

Since 1991, she has been a Faculty Member in the Department of Electrical and Computer Engineering, CSU, where she is currently a Professor. She is engaged in the growth and characterization of metal-oxide materials for the engineering of interference coatings for high-power lasers. She is also actively involved in using bright coherent beams of light of wavelengths between 10 and 50 nm for optics applications such as imaging and ablation.

Dr. Menoni and her team received an "R&D 100 Award" for the invention of a table-top 46.9 nm wavelength microscope that can capture images in a single 1 ns with wavelength spatial resolution in 2008. She is a Fellow of the American Physical Society and the Optical Society of America. She has served the IEEE Photonics Society as a member of the Board of Governors and Vice-President for Publications. She is currently the Editor-in-Chief for the IEEE PHOTONICS JOURNAL.